Original Article | Nuclear Medicine

eISSN 2005-8330
https://doi.org/10.3348/kjr.2021.0455
Korean J Radiol 2022;23(1):112-123

Korean Journal of Radiology
KJR

Relationship between ^{18}F-FDG PET/CT Semi-Quantitative Parameters and International Association for the Study of Lung Cancer, American Thoracic Society/European Respiratory Society Classification in Lung Adenocarcinomas

Lihong Bu[1], Ning Tu[1], Ke Wang[1], Ying Zhou[1], Xinli Xie[2], Xingmin Han[2], Huiqin Lin[3], Hongyan Feng[1]

[1]PET/CT/MRI and Molecular Imaging Center, Renmin Hospital of Wuhan University, Wuhan, China; [2]Department of Nuclear Medicine, The First Affiliated Hospital of Zhengzhou University, Zhengzhou, China; [3]Department of Thoracic Surgery, Renmin Hospital of Wuhan University, Wuhan, China

Objective: To investigate the relationship between ^{18}F-FDG PET/CT semi-quantitative parameters and the International Association for the Study of Lung Cancer, American Thoracic Society/European Respiratory Society (IASLC/ATS/ERS) histopathologic classification, including histological subtypes, proliferation activity, and somatic mutations.

Materials and Methods: This retrospective study included 419 patients (150 males, 269 females; median age, 59.0 years; age range, 23.0–84.0 years) who had undergone surgical removal of stage IA–IIIA lung adenocarcinoma and had preoperative PET/CT data of lung tumors. The maximum standardized uptake values (SUVmax), background-subtracted volume (BSV), and background-subtracted lesion activity (BSL) derived from PET/CT were measured. The IASLC/ATS/ERS subtypes, Ki67 score, and epidermal growth factor/anaplastic lymphoma kinase (EGFR/ALK) mutation status were evaluated. The PET/CT semi-quantitative parameters were compared between the tumor subtypes using the Mann–Whitney U test or the Kruskal–Wallis test. The optimum cutoff values of the PET/CT semi-quantitative parameters for distinguishing the IASLC/ATS/ERS subtypes were calculated using receiver operating characteristic curve analysis. The correlation between the PET/CT semi-quantitative parameters and pathological parameters was analyzed using Spearman's correlation. Statistical significance was set at $p < 0.05$.

Results: SUVmax, BSV, and BSL values were significantly higher in invasive adenocarcinoma (IA) than in minimally IA (MIA), and the values were higher in MIA than in adenocarcinoma in situ (AIS) (all $p < 0.05$). Remarkably, an SUVmax of 0.90 and a BSL of 3.62 were shown to be the optimal cutoff values for differentiating MIA from AIS, manifesting as pure ground-glass nodules with 100% sensitivity and specificity. Metabolic-volumetric parameters (BSV and BSL) were better potential independent factors than metabolic parameters (SUVmax) in differentiating growth patterns. SUVmax and BSL, rather than BSV, were strongly or moderately correlated with Ki67 in most subtypes, except for the micropapillary and solid predominant groups. PET/CT parameters were not correlated with EGFR/ALK mutation status.

Conclusion: As noninvasive surrogates, preoperative PET/CT semi-quantitative parameters could imply IASLC/ATS/ERS subtypes and Ki67 index and thus may contribute to improved management of precise surgery and postoperative adjuvant therapy.

Keywords: *Lung adenocarcinoma; IASLC/ETS/ERS classification; Background-subtracted volume (BSV); Background-subtracted lesion activity (BSL); Maximum standardized uptake value (SUVmax)*

Received: February 22, 2021 **Revised:** August 30, 2021 **Accepted:** September 26, 2021

Corresponding author: Hongyan Feng, MD, PhD, PET/CT/MRI and Molecular Imaging Center, Renmin Hospital of Wuhan University, 95 Zhangzhidong Road, Wuchang District, Wuhan 430060, China.
• E-mail: fenghongyan870625@163.com

Korean Journal of Radiology
KJR

INTRODUCTION

Adenocarcinoma is the most frequent histologic type of lung cancer, accounting for approximately 50% of non-small cell lung cancers (NSCLCs) [1]. The management and prognosis of lung adenocarcinoma depend on stage, histopathologic subtype, proliferation ability, and somatic mutations. According to the National Comprehensive Cancer Network (NCCN) Guideline Version 2.2020, for the treatment of lung adenocarcinoma, curative intent surgery is recommended for stage I–IIIA [2]. Accurate preoperative tumor staging is a prerequisite for successful operation. However, even if patients present with the same TNM stage, the prognosis after surgical resection varies greatly, raising the need for a precise preoperative classification. Together with the advent of personalized surgery and precise postoperative adjuvant therapy, the requirements are even stronger.

Traditional pathological classification has limited direction for surgery or postoperative adjuvant therapy because the terms bronchioloalveolar carcinoma and mixed subtype could not address the complex histological heterogeneity of lung adenocarcinoma [3]. The International Association for the Study of Lung Cancer, American Thoracic Society/European Respiratory Society (IASLC/ATS/ERS) classification made a distinction between preinvasive lesions (adenocarcinoma in situ, AIS) and minimally invasive adenocarcinoma (MIA) and IA, in part presenting substages of adenocarcinoma within the same stage [4]. Furthermore, IA was subclassified by its predominant pattern as lepidic, acinar, papillary, micropapillary, and solid, in part presenting consecutive tumor stepwise progression of lung adenocarcinoma [5]. Furthermore, the IASLC/ETS/ERS classification stressed proliferation activity and gene mutation state testing to improve molecular and prognostic correlations. To date, the IASLC/ETS/ERS classification could be considered a TNM-independent prognostic indicator [6-8], and there is a compelling need to develop preoperative noninvasive imaging surrogates.

Noninvasive ^{18}F-FDG PET/CT imaging of fluorodeoxyglucose is widely used for staging and restaging of lung cancer, as recommended by the NCCN guidelines [2]. The metabolic features and characteristics captured in PET images may also indicate the underlying histopathologic classification associated with tumor biology [9]. Previous studies have demonstrated associations between the maximal standardized uptake value (SUVmax) and IASLC/ATS/ERS subtypes in lung adenocarcinoma [9,10]. However, the results were inconclusive. Some of the reasons may be the fact that the single-voxel-based SUVmax measures demonstrate the tumor pixel with the highest uptake rather than the whole tumor [11-13]. Alternative quantitative metrics that consider not only SUVmax but also tracer uptake throughout the entire lesion have been proposed, such as metabolic tumor volume (MTV), which is defined as the total number of voxels within a volume of interest that have uptake above a predetermined SUV threshold, and total lesion glycolysis (TLG), calculated as MTV x SUVmean. Recent studies have identified volumetric parameters (MTV and TLG) as significant independent variables in predicting histological subtypes of esophageal cancer and other tumors [13-15]. However, MTV or TLG do not consider background activity; therefore, they are not accurate enough to delineate the boundaries of spatial heterogeneity intratumor or metabolically active tumor volume, especially for ground-glass nodules (GGN). Background-subtracted lesion activity (BSL) or background-subtracted volume (BSV) may be more informative to improve histological subtype classification [16-18].

This study aimed to investigate the relationship between PET semi-quantitative parameters (SUVmax, BSV, and BSL) and IASLC/ETS/ERS subtypes, Ki67 scores, and epidermal growth factor (EGFR) or anaplastic lymphoma kinase (ALK) mutation status using surgically resected specimens in a sizable cohort of lung adenocarcinoma.

MATERIALS AND METHODS

Patients

The ethics committee of Renmin Hospital of Wuhan University approved the protocol of this retrospective study and waived the requirement of obtaining informed consent (IRB No. 2019-X-70). From March 2011 to December 2019, consecutive patients with newly diagnosed lung adenocarcinoma who underwent ^{18}F-FDG PET/CT before surgery were enrolled. General and clinicopathological parameters including age, sex, shape of lung lesions, tumor diameter, and clinical TNM stage and IASLC/ATS/ERS histologic subtypes at the initial staging PET/CT examination were obtained.

The inclusion criteria were single pulmonary nodule on PET/CT, high resolution CT (HRCT); thickness: 1 mm, therapeutic tumor resection within 1 month, postoperative pathologic analysis confirming clinical stage IA–IIIA

 https://doi.org/10.3348/kjr.2021.0455

Table 1. General, Clinicopathological and PET/CT Semi-Quantitatively Parameters and EGFR/ALK Mutation Status in 419 IA-IIIA Patients

Characteristics	Total	AIS	MIA	Lepidic Predominant	Acinar Predominant	Papillary Predominant	Micropapillary Predominant	Solid Predominant	Variant
Number of patients	419	22 (5.3)	37 (8.8)	60 (14.3)	202 (48.2)	22 (5.3)	8 (1.9)	30 (7.2)	38 (9.1)
Age*, year	59 (23–84)	57 (51–66)	55 (33–69)	61 (23–78)	60 (32–84)	61 (51–72)	50 (38–71)	61 (48–74)	63 (44–80)
Sex									
Male	150 (35.8)	0	6	22	72	8	2	22	18
Female	269 (64.2)	22	31	38	130	14	6	8	20
TNM stage									
IA	303 (72.3)	22	37	46	154	6	4	14	20
IB + IIA	44 (10.5)	0	0	6	20	8	2	2	6
IIB + IIIA	72 (17.2)	0	0	8	28	8	2	14	12
Lung lesion shape									
Pure GGN	37 (8.8)	16	9	8	4	0	0	0	0
Subsolid nodule	54 (12.9)	3	11	18	18	2	0	0	2
Solid nodule	238 (56.8)	3	17	28	144	4	4	20	18
Mass	90 (21.5)	-	-	6	36	16	4	10	18
Tumor size*, cm	2.0 (0.4–7.5)	0.9 (0.4–1.6)	1.1 (0.6–1.4)	1.8 (0.9–5.1)	2.1 (0.9–4.6)	4.0 (1.1–6.6)	3.2 (2.0–3.6)	2.7 (1.1–5.7)	2.5 (1.3–7.5)
PET/CT									
SUVmax*	4.2 (0.6–20.5)	0.7 (0.6–2.3)	1.4 (0.7–5.5)	2.4 (0.7–14.5)	6.3 (1.4–20.2)	4.3 (1.95–13.1)	14.2 (4.7–19.2)	12.2 (3.3–20.5)	5.7 (2.2–20.3)
BSV*, cm^3	6.5 (0.6–166)	1.0 (0.7–7.5)	3.2 (0.6–14.1)	8.8 (2.0–26.7)	6.2 (1.1–39.3)	14.6 (4.8–71.1)	10.6 (2.8–14.7)	13.4 (1.0–33.3)	17.5 (3.4–166.0)
BSL (x 10^3)*, g	14.6 (1.2–188.6)	1.4 (1.3–7.8)	6.2 (1.2–15.4)	9.0 (2.9–88.3)	16.8 (1.8–172.3)	35.2 (7.2–189.0)	36.0 (28.8–152.2)	47.3 (5.1–286.4)	25.0 (5.5–188.6)
Ki67, %									
Absolute value*	18.2 (1–88)	4.8 (1–10)	7.8 (5–20)	10.0 (2–30)	19.4 (1–88)	9.4 (2–30)	16.3 (2–30)	25.1 (1–60)	20.1 (2–80)
Ki67 > 20	113 (27.0)	0	3	4	38	2	4	16	8
Ki67 ≤ 20	306 (73.0)	11	6	42	124	18	4	14	22
EGFR									
Wild-type	41/194 (21.1)	3/8 (37.5)	2/20 (10)	0/16 (0)	18/104 (17.3)	0/12 (0)	2/8 (25)	4/8 (50)	12/18 (66.7)
Mutant	153/194 (78.9)	5/8 (62.5)	18/20 (90)	16/16 (100)	86/104 (82.7)	12/12 (100)	6/8 (75)	4/8 (50)	6/18 (33.3)
ALK									
Negative	277/287 (96.5)	20/20 (100)	27/27 (100)	26/26 (100)	144/146 (98.6)	14/14 (100)	6/6 (100)	18/18 (100)	22/30 (73.3)
Positive	10/287 (3.5)	0/20 (0)	0/27 (0)	0/26 (0)	2/146 (1.4)	0/14 (0)	0/6 (0)	0/18 (0)	8/30 (26.7)

*Data are medians with ranges in parentheses. Otherwise, data are the number of patients with percentages in parentheses. AIS = adenocarcinoma in situ, ALK = anaplastic lymphoma kinase, BSL = background subtracted lesion activity, BSV = background subtracted volume, EGFR = epidermal growth factor receptor, GGN = ground-glass nodule, MIA = minimally invasive adenocarcinoma, SUVmax = maximum standardized uptake value

https://doi.org/10.3348/kjr.2021.0455

Korean Journal of Radiology
KJR

adenocarcinoma, and no history of severe liver disease, diabetes mellitus, or cancer. The exclusion criteria were any antitumor therapy, lesions that were difficult to measure, or poor image quality. A total of 527 patients were initially enrolled, and 108 patients were excluded from the analysis; 95 received antitumor treatment, eight had lesions that were difficult to measure, and five had poor image quality. A total of 419 patients were included in the study.

^{18}F-FDG PET/CT Acquisition and Imaging Evaluation

All patients underwent staging ^{18}F-FDG PET/CT before surgery (see Supplement for details). All PET/CT and HRCT images were visually and semi-quantitatively reviewed independently by two experienced nuclear medicine physicians and radiologists with many years of experience in chest image interpretation and general PET/CT on an Advantage Workstation (AW) 4.6 postprocessing workstation. A consensus was reached by discussion with two more experienced nuclear medicine physicians and one thoracic specialist in case of disagreement. The percentage of disagreement between the two readers was 10.9%.

Considering the impact of background, location of the lesion, motion artifacts, or image noise, the metabolic active volume of the primary tumor was delineated using a background-adaptive method as previously reported [18-22]. Within the selected volume of interest, BSV and BSL were computed automatically using a GE AW 4.6. Tumor dimensions and morphological features were extracted from the HRCT images.

Histological Confirmation, Tumor Grading, and Molecular Analysis

Primary tumor resection specimens were used to determine each tumor's histological subtype, the immunohistochemical index ratio of Ki67 (Ki67%), EGFR, and ALK mutation status using SNaPshot [23]. Histological subtypes of lung adenocarcinoma were classified according to the 2011 IASLC/ATS/ERS classification. Tumor staging at diagnosis was determined based on surgical pathology and PET/CT images. Ki67 is a nuclear protein common to proliferating human cells and can be detected immunohistochemically using the monoclonal antibody MIB-1. Advanced genetic analysis of the EGFR and ALK mutations, which were classified as positive or negative, was available in a subgroup of 194 and 287 patients, respectively. See Supplement for further details.

Statistical Analysis

Statistical analysis was performed using IBM SPSS Statistics for Windows (version 23.0; IBM Corp.). Qualitative variables were summarized using percentages, frequency, and quantitative variables using mean ± standard deviation.

Table 2. Association between Clinicopathological Variables and PET/CT Semi-Quantitative Parameters

Characteristics	SUVmax	*P*	BSV	*P*	BSL	*P*
Sex		< 0.001		0.098		< 0.001
Male	7.9 ± 5.1		13.8 ± 21.9		80.8 ± 225.9	
Female	5.1 ± 4.6		10.3 ± 13.4		31.0 ± 66.0	
Tumor stage		< 0.001		< 0.001		< 0.001
IA	4.5 ± 3.9		6.9 ± 6.7		14.6 ± 18.2	
IB + IIA	7.6 ± 4.7		19.6 ± 8.8		72.2 ± 58.9	
IIB + IIIA	11.9 ± 4.6		26.4 ± 33.3		177.8 ± 318.2	
Tumor size, cm		< 0.001		< 0.001		< 0.001
≤ 3	4.9 ± 4.1		7.0 ± 6.4		17.7 ± 20.8	
> 3	10.1 ± 5.4		29.3 ± 29.3		169.4 ± 293.0	
Lymphatic metastasis		< 0.001		0.123		< 0.001
Negative	5.0 ± 4.3		11.5 ± 17.9		44.2 ± 159.0	
Positive	11.2 ± 4.5		11.7 ± 12.4		68.9 ± 70.2	
Lung lesion patterns		< 0.001		0.000		0.000
Pure GGN	1.3 ± 0.7		4.7 ± 6.6		6.4 ± 7.0	
Subsolid nodules	2.3 ± 2.1		9.8 ± 8.5		11.3 ± 10.8	
Solid nodule	5.9 ± 4.1		6.9 ± 6.1		18.5 ± 17.8	
Mass	11.1 ± 5.0		27.7 ± 29.2		168.9 ± 285.7	

Data are mean ± standard deviation. BSL = background subtracted lesion activity, BSV = background subtracted volume, GGN = ground-glass nodule, SUVmax = maximum standardized uptake value

 https://doi.org/10.3348/kjr.2021.0455

Comparisons were performed using the Mann–Whitney U test to compare two groups and the Kruskal–Wallis test to compare multiple groups. The optimum cutoff point of PET/CT semi-quantitative parameters was calculated using the receiver operating characteristic curve analysis to differentiate between the IASLC/ATS/ERS subtypes. Spearman's coefficient was used for the correlation analysis. Statistical significance was set at $p < 0.05$.

RESULTS

General, Clinicopathological, and PET/CT Semi-Quantitative Parameters and EGFR/ALK Mutation Status

Demographic data, clinicopathological, and PET/CT semi-quantitative parameters in 419 IA–IIIA lung adenocarcinoma patients with different subtypes are summarized in Table 1. In detail, 419 lung adenocarcinoma lesions (37 pure GGN, 54 subsolid nodules, 238 solid nodules, and 90 mass-forming) were included from 419 patients (150 males, 269 females; median age: 59.0 years; range, 23.0–84.0 years). The median diameter of the tumor was 2.0 cm (range, 0.4–7.5 cm). The tumor stage was as follows: stage I (n = 329, 78.5%) (IA1: n = 40; IA2: n = 175; IA3: n = 88; IB: n = 26), stage II (n = 46, 11.0%) (IIA: n = 18; IIB: n = 28), and stage IIIA (n = 44, 10.5%). The 419 tumors can be categorized into one of the subtypes of adenocarcinoma (22 AIS, 37 MIA, 322 IA, and 38 variants of IA, including seven intestinal adenocarcinomas and 31 mucinous adenocarcinomas). IA lesions were subclassified into the following subtypes: 60 (18.6%) lepidic-dominant adenocarcinoma, 202 (62.7%) acinar-dominant adenocarcinoma, 22 (6.8%) papillary-dominant adenocarcinoma, 30 (9.3%) solid-dominant adenocarcinoma, and 8 (2.5%) micropapillary adenocarcinoma. The median value of the hotspot Ki67 index was 17.4% (range, 1%–88%). ^{18}F-FDG PET/CT was performed before the operation in a median of 14 days (range, 1–30 days). The median SUVmax was 4.2 (range, 0.6–20.5), the median BSV was 6.5 cm^3 (range, 0.6–166.0 cm^3), and the median BSL was 14.6 x 10^3 g (range, 1.2 x 10^3–188.6 x 10^3 g).

Association between Clinicopathological Variables and PET/CT Semi-Quantitative Parameters

We investigated the influence of clinicopathological factors on PET/CT semi-quantitative parameters (Table 2) and found that all clinicopathological parameters (except age) were significantly associated with SUVmax, BSV, and BSL. In detail, all variables were higher in males, in large-diameter pulmonary lesions (≥ 3 cm), compared with their corresponding cohorts. All variables of PET/CT semi-quantitative parameters increased with tumor stage. According to the shape of the lesions, the values of SUVmax, BSV, and BSL went as mass > solid nodules > subsolid nodules > pure GGN. Almost all clinicopathological variables could be interpreted by differences in tumor stage and classification.

Comparison of PET/CT Semi-Quantitative Parameters between IASLC/ATS/ERS Subgroups

We evaluated the association of PET/CT semi-quantitative

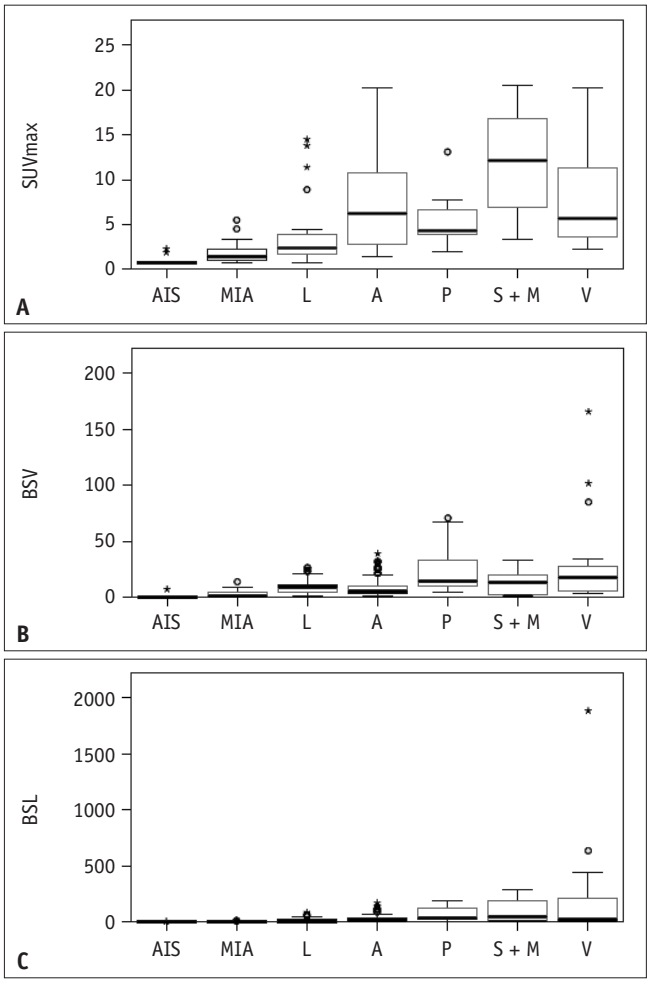

Fig. 1. Box plots showing the distribution of semi-quantitatively parameters of PET/CT associated with the histological subtype of adenocarcinoma (A-C). A = acinar predominant adenocarcinoma, AIS = adenocarcinoma in situ, BSL = background subtracted lesion activity, BSV = background subtracted volume, L = lepidic predominant adenocarcinoma, MIA = minimally invasive adenocarcinoma, P = papillary predominant adenocarcinoma, SUVmax = maximum standardized uptake value, S + M = solid and micropapillary predominant adenocarcinoma, V = variant adenocarcinoma

https://doi.org/10.3348/kjr.2021.0455

Korean Journal of Radiology
KJR

Table 3. Pairwise Comparisons of PET Semi-Quantitatively Parameters between Different Subgroups

Subgroups	SUVmax		BSV		BSL	
	Mean	*P*	Mean	*P*	Mean	*P*
AIS vs. MIA	1.0 vs. 1.9	0.001	1.6 vs. 4.5	< 0.001	2.1 vs. 6.9	< 0.001
AIS vs. IA	1.0 vs. 6.8	0.000	1.6 vs. 10.9	< 0.001	2.1 vs. 37.8	< 0.001
MIA vs. IA	1.9 vs. 6.8	0.000	4.5 vs. 10.9	< 0.001	6.9 vs. 37.8	< 0.001
AIS vs. L	1.0 vs. 3.7	0.000	1.6 vs. 10.5	< 0.001	2.1 vs. 18.9	< 0.001
MIA vs. L	1.9 vs. 3.7	0.005	4.5 vs. 10.5	< 0.001	6.9 vs. 18.9	0.005
M vs. S	13.1 vs. 11.3	0.413	14.3 vs. 9.7	0.907	106.1 vs. 63.2	0.516
L vs. A	3.7 vs. 6.9	0.000	10.5 vs. 9.0	0.073	18.9 vs. 29.0	0.015
L vs. P	3.7 vs. 5.3	0.059	10.5 vs. 25.7	0.005	18.9 vs. 67.3	< 0.001
L vs. S + M	3.7 vs. 11.7	0.000	10.5 vs. 13.4	0.038	18.9 vs. 97.1	< 0.001
L vs. V	3.7 vs. 7.9	0.000	10.5 vs. 30.9	0.019	18.9 vs. 209.9	< 0.001
A vs. P	6.9 vs. 5.3	0.107	9.0 vs. 12.3	< 0.001	29.0 vs. 67.3	0.003
A vs. S + M	6.9 vs. 11.7	0.000	9.0 vs. 13.4	0.008	29.0 vs. 97.1	< 0.001
A vs. V	6.9 vs. 7.9	0.231	9.0 vs. 30.9	< 0.001	29.0 vs. 209.9	0.002
P vs. S + M	5.3 vs. 11.7	0.000	25.7 vs. 13.4	0.385	67.3 vs. 97.1	0.932
P vs. V	5.3 vs. 7.9	0.052	25.7 vs. 30.9	0.433	67.3 vs. 209.9	0.689
S + M vs. V	11.7 vs. 7.9	0.004	13.4 vs. 30.9	0.066	97.1 vs. 209.9	0.713

A = acinar predominant adenocarcinoma, AIS = adenocarcinoma in situ, BSL = background subtracted lesion activity, BSV = background subtracted volume, L = lepidic predominant adenocarcinoma, M = micropapillary adenocarcinoma, MIA = minimally invasive adenocarcinoma, P = papillary predominant adenocarcinoma, S = solid predominant adenocarcinoma, SUVmax = maximum standardized uptake value, S + M = solid predominant and micropapillary adenocarcinoma, V = variant adenocarcinoma

parameters and the degree of tumor invasiveness (Fig. 1, Table 3), and found that SUVmax, BSV, and BSL values were significantly higher in IA (median: SUVmax, 6.8; BSV, 10.9 cm^3; BSL, 37.8 x 10^3 g) than in MIA (median: SUVmax, 1.9; BSV, 4.5 cm^3; BSL, 6.9 x 10^3 g), and the latter were higher than those in AIS (median: SUVmax, 1.0; BSV, 1.6 cm^3; BSL, 2.1 x 10^3 g; all $p < 0.05$) (Fig. 2, Table 3).

Furthermore, PET/CT semi-quantitative parameters were compared between the different growth patterns (Supplementary Fig. 1, Tables 3, 4). All lepidic growth subtypes, including AIS, MIA, and lepidic predominant adenocarcinoma, had significantly lower SUVmax, BSV, and BSL values than the invasive non-lepidic growth subtypes (all $p < 0.05$) (Table 3). Lepidic predominant adenocarcinoma has the lowest SUVmax, BSV and BSL values, while solid predominant or micropapillary adenocarcinoma has the highest among invasive growth pattern-specific subtypes. PET/CT semi-quantitative parameters in AIS or MIA were lower than those in the lepidic predominant group ($p < 0.01$) (Table 3). Remarkably, an SUVmax of 0.90 and a BSL of 3.62 x 10^3 g were shown to be the optimal cutoff values to differentiate MIA from AIS that manifest as pure GGN with 100% sensitivity and specificity, with an area under the curve (AUC) of 1 (Table 4).

As presented in Table 3, volumetric parameters (BSV and BSL) were better potential independent factors than metabolic parameters (SUVmax) to distinguish growth patterns, especially for well-differentiated (AIS, MIA) or moderately differentiated adenocarcinoma (lepidic predominant, acinar predominant, papillary predominant) (all $p < 0.05$). However, SUVmax, BSV, and BSL could not distinguish between poorly differentiated (solid predominant and micropapillary adenocarcinoma) and papillary predominant.

We noticed that BSV and BSL could discriminate between acinar predominant and papillary predominant subtypes (AUC_{BSV} = 0.804; AUC_{BSL} = 0.718), which have similar biological behaviors.

However, the data for the variant subtypes were complicated. It was clear that the variant adenocarcinoma had a higher BSV than any other histological subtype, although no statistically significant differences were observed between the papillary predominant and variant groups (Supplementary Fig. 2, Table 3). Combining its significantly high BSV with inherent PET/CT imaging features may provide an important reference for the diagnosis of variant adenocarcinomas.

Correlation between PET/CT Semi-Quantitative Parameters and Proliferation Index Ki67 in Primary Tumors

Table 5 shows Spearman's rank correlation results between the PET/CT semi-quantitative parameters and Ki67 value. In

 https://doi.org/10.3348/kjr.2021.0455

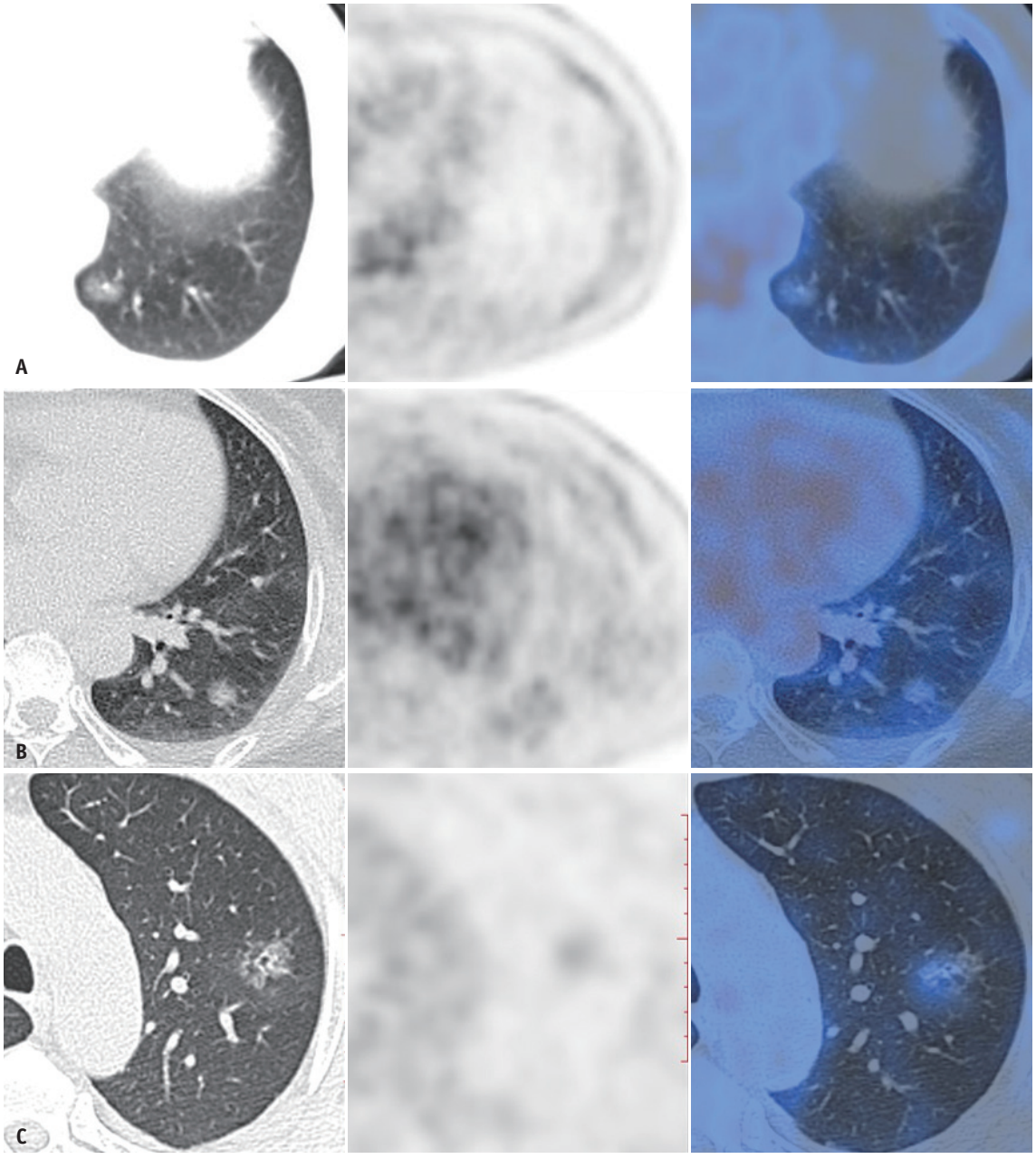

Fig. 2. CT, PET, and PET/CT of AIS, MIA and invasive adenocarcinoma with low FDG uptake.
A-C. Axial HRCT scan, PET, and PET/CT of adenocarcinoma in situ **(A)**, minimally invasive adenocarcinoma **(B)**, and invasive adenocarcinoma with predominant lepidic pattern **(C)** manifesting as pure ground-glass nodule with maximum standardized uptake value values of 0.7, 1.2, and 1.5, respectively. The corresponding Ki67 index of each subtype of lepidic growth subtype is 5%, 10%, and 15%, respectively.

all patients, semi-quantitative parameters (SUVmax, BSL, and BSV) derived from PET/CT were moderately or weakly related to the Ki67 value (ρ = 0.529, 0.375, and 0.474, respectively; $p < 0.001$). Metabolic parameters (SUVmax), rather than volumetric parameters (BSL and BSV), were correlated with Ki67 in almost all subtypes, except MIA (all $p > 0.05$). Impressively, BSV and BSL did not have a correlation with Ki67 in the micropapillary + solid predominant group.

Association between PET/CT Semi-Quantitative Parameters and EGFR/ALK Mutations in Primary Tumors

As shown in Table 1, the EGFR and ALK mutation rates were 78.9% and 3.5%, respectively. The rates according to the IASLC/ATS/ERS histological classification are also provided in Table1. We did not find any association

https://doi.org/10.3348/kjr.2021.0455

Korean Journal of Radiology
KJR

Table 4. Receiver Operating Characteristic Curve Analysis of Different PET Semi-Quantitative Parameters in Differentiating Histological Subgroups

Different Group	SUVmax				BSV				BSL			
	AUC	Sensitivity (%)	Specificity (%)	Cutoff	AUC	Sensitivity (%)	Specificity (%)	Cutoff	AUC	Sensitivity (%)	Specificity (%)	Cutoff
AIS vs. MIA	0.850	91.9	81.8	0.87	0.647	61.4	90.9	1.58	0.882	94.6	90.9	2.21
AIS vs. MIA (pure GGN)	1.000	100	100	0.90	0.767	75.7	100	1.03	1.000	100	100	3.62
MIA vs. L	0.716	86.7	54.1	1.45	0.858	96.7	64.9	2.27	0.684	62.0	75.7	7.30
L vs. A	0.742	56.4	86.7	4.55	0.591	63.3	59.4	7.12	0.615	74.3	50.0	8.14
A vs. P	0.548	47.5	81.8	6.80	0.804	81.8	73.3	10.03	0.718	81.8	60.4	22.40
P vs. S + M	0.871	84.2	81.8	6.70	0.670	100	31.6	3.94	0.541	36.3	100	189.96

A = acinar predominant adenocarcinoma, AIS = adenocarcinoma in situ, AUC = area under the curve, BSL = background subtracted lesion activity, BSV = background subtracted volume, GGN = ground-glass nodule, L = lepidic predominant adenocarcinoma, MIA = minimally invasive adenocarcinoma, P = papillary predominant adenocarcinoma, SUVmax = maximum standardized uptake value, S + M = solid predominant and micropapillary adenocarcinoma

between PET/CT semi-quantitative parameters and EGFR/ALK mutation status (Supplementary Table 1). There was no significant difference in PET/CT semi-quantitative parameters between the EGFR wild-type and EGFR mutant groups or between the ALK-positive and-negative groups.

DISCUSSION

According to the IASLC/ATS/ERS classification, lung adenocarcinoma is classified into more specific types and subtypes with different degrees of invasion and growth patterns, which present consecutive substages of lung adenocarcinoma. This spectrum of subtypes can be translated into various PET/CT presentations and features.

In this study, we found that PET semi-quantitative parameters can be used as noninvasive imaging surrogates to distinguish between MIA and IA (Fig. 2), which is consistent with several previous studies [24-26]. Notably, PET semi-quantitative parameters have the capability to differentiate AIS from MIA ($p < 0.05$), especially for persistent pure GGN lesions. Generally, on HRCT images, persistent pure GGN lesions are believed to correspond mainly to AIS and MIA in IALSC/ATS/ERS adenocarcinoma classification studies [27,28]; however, the difference in PET parameters was not so definite. In this study, SUVmax, BSV, and BSL values were significantly higher in the MIA group than in the AIS group (Fig. 1, Table 3). An SUVmax of 0.90 and a BSL of 3.62 were shown to be the optimal cutoff values to differentiate MIA from AIS manifesting as pure GGN with 100% sensitivity and specificity. Our analysis yielded the highest AUCs of 1.0 in the aforementioned studies. Our result is not aligned with the previous study by Nakamura et al. [10], in which there were no significant differences in SUVmax between the MIA and AIS groups. One possible reason is that the number of patients included in the study by Nakamura et al. [10] was not large enough compared with our study. Their study included 14 patients with MIA and 12 patients with AIS, while our cohort included 37 patients with MIA and 22 patients with AIS. Another possible reason is that we implemented a more accurate background-adaptive method to determine SUVmax, BSL, and BSV, in which tumor activity is considered regardless of location. Preoperative discrimination between AIS and MIA by PET/CT may help in the choice of operation method. Limited resection, the "sublobar" resection comprising anatomical segmentectomy or wedge excision, is recommended for AIS lesions, while

https://doi.org/10.3348/kjr.2021.0455

Table 5. Correlation between Semi-Quantitatively Parameters of PET/CT and Ki67 Scores for Histological Subtypes

Characteristics	Ki67 (Median, Range)	Correlation with Ki67*		
		SUVmax	BSV	BSL
AIS	4.8 (1–10)	0.818 (0.002)	0.131 (0.670)	0.229 (0.452)
MIA	7.8 (5–20)	-0.281 (0.465)	-0.205 (0.568)	-0.115 (0.768)
Lepidic	10.0 (2–30)	0.360 (0.014)	0.401 (0.006)	0.459 (0.001)
Acinar	19.4 (1–88)	0.481 (< 0.001)	0.296 (0.007)	0.584 (< 0.001)
Papillary	9.4 (2–30)	0.778 (< 0.001)	-0.393 (0.087)	-0.215 (0.362)
Micropapillary + solid	16.3 (2–30)	0.361 (0.024)	-0.366 (0.163)	0.073 (0.788)
Variants	20.1 (2–80)	0.440 (0.015)	0.527 (0.003)	0.577 (0.001)
All	18.2 (1–88)	0.529 (< 0.001)	0.375 (< 0.001)	0.474 (< 0.001)

*Data are Spearman correlation coefficients with the corresponding *p* values in parentheses. AIS = adenocarcinoma in situ, BSL = background subtracted lesion activity, BSV = background subtracted volume, MIA = minimally invasive adenocarcinoma, SUVmax = maximum standardized uptake value

segmentectomy is recommended for MIA lesions. Regarding IA, lobectomy and systematic nodal dissection are generally recommended regardless of the IASLC/ATS/ERS classification subtypes.

We also observed the highest SUVmax in solid predominant adenocarcinoma and the lowest in lepidic predominant adenocarcinoma when investigating the five subtypes of IA, which is consistent with previous studies [29,30]. We also observed another impressive finding that BSV and BSL were better potential independent factors than SUVmax in differentiating growth patterns. Strong evidence to support the conclusion is that BSV and BSL values may be sufficient to differentiate acinar predominant from papillary predominant ($p < 0.05$), which are indistinguishable from SUVmax. Furthermore, our results showed that BSV in variant adenocarcinoma was significantly higher than in the others, which was first reported. The reasons may be partially due to tumor heterogeneity, partial volume effect, and biological tumor volume may hinder the exact assessment of tumor characteristics using SUVmax. Tumor invasiveness, heterogeneity, and cellularity as determinants of growth patterns could be reflected by biological tumor volume [15,31,32]. The metabolo-volumetric parameters, especially BSV, show the metabolically active component through the tumor volume and accurately define the biological tumor volume on PET images.

In many previous studies, SUVmax was reported to be positively correlated with Ki67 expression in patients with NSCLC [33-35]. However, no studies have focused on the correlation between glucose metabolism and Ki67 in lung adenocarcinoma. This study represents the relationship between the Ki67 score and ^{18}F-FDG uptake in lung adenocarcinoma across IASLC/ETS/ERS subtypes. Our results suggested that metabolic parameters (SUVmax) were moderately correlated with the Ki67 index (mean and hotspot), whereas volumetric PET parameters (BSV) showed a weaker correlation. This effect is possibly due to the increased glucose uptake in highly proliferative cancers, resulting in high levels of SUVmax. Consistent with our findings, a high ^{18}F-FDG avidity (SUVmax) was reported to be significantly associated with a high Ki67 index in breast cancer [36-38], gliomas [39], and lymphoma [40]. When analyzing different histological subtypes, we found that better-differentiated lung adenocarcinoma (papillary, acinar, lepidic adenocarcinoma, and variant adenocarcinoma) had a better correlation between Ki67 and PET semi-quantitative parameters than more poorly differentiated ones (micropapillary and solid predominant adenocarcinoma). The results may be explained by the higher intratumor heterogeneity, higher complexity of the intertumor microenvironment, and intercomponents in poorly differentiated adenocarcinoma.

Previous studies have investigated positive associations between PET semi-quantitative parameters and EGFR/ALK mutations in NSCLC [41-43], including adenocarcinoma [44,45]. In this study, our results on the distribution of the EGFR and ALK mutation status of each lung adenocarcinoma subtype are in line with those of other studies [46]. However, we found contradictory results from previous reports that PET semi-quantitative parameters were not correlated with EGFR/ALK mutation status in lung adenocarcinoma. Some of the reasons may be the result of highly heterogeneous histological subgroups. The relationship between EGFR mutation status and metabolic activity in lung adenocarcinoma needs to be validated in a larger cohort or a multicenter study.

https://doi.org/10.3348/kjr.2021.0455

Korean Journal of Radiology
KJR

This study had some limitations. First, although this study included over 400 patients, the sample size of each group was not large enough. In the future, we need to continuously increase the sample size to give much more power to the ^{18}F-FDG metabolic characteristics to identify each IASLC/ATS/ERS lung adenocarcinoma subtype. Second, the clinical implications of preoperative prediction of IASLC/ATS/ERS classification using ^{18}F-FDG PET/CT semi-quantitative parameters in guiding postoperative neoadjuvant therapy need to be validated in a large cohort in the future.

In conclusion, PET/CT semi-quantitative parameters can differentiate AIS, MIA, and IA. Volumetric parameters (BSV) and metabolic parameters (SUVmax) may reflect different growth patterns across subtypes and proliferative activity, respectively, while metabolo-volumetric parameters (BSL) may reflect both well. As noninvasive surrogates, preoperative PET/CT semi-quantitative parameters could imply IASLC/ATS/ERS subtypes and Ki67 index and thus may contribute to improved management of precise surgery and postoperative adjuvant therapy.

Supplement

The Supplement is available with this article at https://doi.org/10.3348/kjr.2021.0455.

Availability of Data and Material

The datasets generated or analyzed during the study are available from the corresponding author on reasonable request.

Conflicts of Interest

The authors have no potential conflicts of interest to disclose.

Author Contributions

Conceptualization: all authors. Data curation: Ke Wang, Ying Zhou, Hongyan Feng. Formal analysis: Ke Wang, Ning Tu, Hongyan Feng, Lihong Bu. Investigation: Hongyan Feng. Methodology: Ke Wang, Hongyan Feng. Validation: Hongyan Feng. Writing—original draft: Hongyan Feng, Lihong Bu. Writing—review & editing: Lihong Bu.

ORCID iDs

Lihong Bu
https://orcid.org/0000-0002-1102-3158
Ning Tu
https://orcid.org/0000-0002-8845-9689
Ke Wang
https://orcid.org/0000-0003-0379-876X
Ying Zhou
https://orcid.org/0000-0003-0408-3731
Xinli Xie
https://orcid.org/0000-0003-1487-7527
Xingmin Han
https://orcid.org/0000-0002-4069-6095
Huiqin Lin
https://orcid.org/0000-0003-1340-6109
Hongyan Feng
https://orcid.org/0000-0003-1352-3196

Funding Statement

This work was supported in part, by the National Science Foundation of China (81871419 to Dr. Bu, 81701735 to Dr. Feng), Seed project in Sino foreign joint research platform of Wuhan University (2309-413100006 to Dr. Bu), Hubei Provincial Natural Science Foundation of China (2017CFB781 to Dr. Bu), Chinese Society of Clinical Oncology Foundation (Y-HR2016-44 to Dr. Bu), Hubei Provincial Health Department (WJ2017M012 to Dr. Bu) and Young Teachers' Independent Research Funding of Wuhan University (2042019kf0054 to Dr. Tu). This was not an industry supported study.

REFERENCES

1. Bray F, Ferlay J, Soerjomataram I, Siegel RL, Torre LA, Jemal A. Global cancer statistics 2018: GLOBOCAN estimates of incidence and mortality worldwide for 36 cancers in 185 countries. *CA Cancer J Clin* 2018;68:394-424
2. Ettinger DS, Wood DE, Aggarwal C, Aisner DL, Akerley W, Bauman JR, et al. NCCN guidelines insights: non-small cell lung cancer, version 1.2020. *J Natl Compr Canc Netw* 2019;17:1464-1472
3. Travis WD, Brambilla E, Nicholson AG, Yatabe Y, Austin JHM, Beasley MB, et al. The 2015 World Health Organization classification of lung tumors: impact of genetic, clinical and radiologic advances since the 2004 classification. *J Thorac Oncol* 2015;10:1243-1260
4. Travis WD, Brambilla E, Noguchi M, Nicholson AG, Geisinger KR, Yatabe Y, et al. International association for the study of lung cancer/american thoracic society/european respiratory society international multidisciplinary classification of lung adenocarcinoma. *J Thorac Oncol* 2011;6:244-285
5. Noguchi M. Stepwise progression of pulmonary

adenocarcinoma--clinical and molecular implications. *Cancer Metastasis Rev* 2010;29:15-21
6. Fang W, Xiang Y, Zhong C, Chen Q. The IASLC/ATS/ERS classification of lung adenocarcinoma-a surgical point of view. *J Thorac Dis* 2014;6:S552-S560
7. Van Schil PE, Asamura H, Rusch VW, Mitsudomi T, Tsuboi M, Brambilla E, et al. Surgical implications of the new IASLC/ATS/ERS adenocarcinoma classification. *Eur Respir J* 2012;39:478-486
8. Zugazagoitia J, Enguita AB, Nuñez JA, Iglesias L, Ponce S. The new IASLC/ATS/ERS lung adenocarcinoma classification from a clinical perspective: current concepts and future prospects. *J Thorac Dis* 2014;6:S526-S536
9. Chiu CH, Yeh YC, Lin KH, Wu YC, Lee YC, Chou TY, et al. Histological subtypes of lung adenocarcinoma have differential 18F-fluorodeoxyglucose uptakes on the positron emission tomography/computed tomography scan. *J Thorac Oncol* 2011;6:1697-1703
10. Nakamura H, Saji H, Shinmyo T, Tagaya R, Kurimoto N, Koizumi H, et al. Close association of IASLC/ATS/ERS lung adenocarcinoma subtypes with glucose-uptake in positron emission tomography. *Lung Cancer* 2015;87:28-33
11. Satoh Y, Onishi H, Nambu A, Araki T. Volume-based parameters measured by using FDG PET/CT in patients with stage I NSCLC treated with stereotactic body radiation therapy: prognostic value. *Radiology* 2014;270:275-281
12. Boellaard R. Standards for PET image acquisition and quantitative data analysis. *J Nucl Med* 2009;50 Suppl 1:11S-20S
13. Zhu L, Li X, Wang J, Fu Q, Liu J, Ma W, et al. Value of metabolic parameters in distinguishing primary mediastinal lymphomas from thymic epithelial tumors. *Cancer Biol Med* 2020;17:468-477
14. Korkmaz U, Hacioglu MB, Kostek O, Sut N, Kodaz H, Erdogan B, et al. The relationship between FDG PET/CT-defined metabolic parameters and the histopathological subtype of oesophageal carcinomas. *Pol J Radiol* 2020;85:e254-e260
15. Husby JA, Reitan BC, Biermann M, Trovik J, Bjørge L, Magnussen IJ, et al. Metabolic tumor volume on 18F-FDG PET/CT improves preoperative identification of high-risk endometrial carcinoma patients. *J Nucl Med* 2015;56:1191-1198
16. Liao S, Penney BC, Wroblewski K, Zhang H, Simon CA, Kampalath R, et al. Prognostic value of metabolic tumor burden on 18F-FDG PET in nonsurgical patients with non-small cell lung cancer. *Eur J Nucl Med Mol Imaging* 2012;39:27-38
17. Chen HH, Chiu NT, Su WC, Guo HR, Lee BF. Prognostic value of whole-body total lesion glycolysis at pretreatment FDG PET/CT in non-small cell lung cancer. *Radiology* 2012;264:559-566
18. Burger IA, Vargas HA, Apte A, Beattie BJ, Humm JL, Gonen M, et al. PET quantification with a histogram derived total activity metric: superior quantitative consistency compared to total lesion glycolysis with absolute or relative SUV thresholds in phantoms and lung cancer patients. *Nucl Med Biol* 2014;41:410-418
19. Burger IA, Vargas HA, Beattie BJ, Goldman DA, Zheng J, Larson SM, et al. How to assess background activity: introducing a histogram-based analysis as a first step for accurate one-step PET quantification. *Nucl Med Commun* 2014;35:316-324
20. Burger IA, Casanova R, Steiger S, Husmann L, Stolzmann P, Huellner MW, et al. 18F-FDG PET/CT of non-small cell lung carcinoma under neoadjuvant chemotherapy: background-based adaptive-volume metrics outperform TLG and MTV in predicting histopathologic response. *J Nucl Med* 2016;57:849-854
21. Xu W, Yu S, Ma Y, Liu C, Xin J. Effect of different segmentation algorithms on metabolic tumor volume measured on 18F-FDG PET/CT of cervical primary squamous cell carcinoma. *Nucl Med Commun* 2017;38:259-265
22. Wang XY, Zhao YF, Liu Y, Yang YK, Zhu Z, Wu N. Comparison of different automated lesion delineation methods for metabolic tumor volume of 18F-FDG PET/CT in patients with stage I lung adenocarcinoma. *Medicine (Baltimore)* 2017;96:e9365
23. Dias-Santagata D, Akhavanfard S, David SS, Vernovsky K, Kuhlmann G, Boisvert SL, et al. Rapid targeted mutational analysis of human tumours: a clinical platform to guide personalized cancer medicine. *EMBO Mol Med* 2010;2:146-158
24. Qi L, Lu W, Yang L, Tang W, Zhao S, Huang Y, et al. Qualitative and quantitative imaging features of pulmonary subsolid nodules: differentiating invasive adenocarcinoma from minimally invasive adenocarcinoma and preinvasive lesions. *J Thorac Dis* 2019;11:4835-4846
25. Eriguchi D, Shimada Y, Imai K, Furumoto H, Okano T, Masuno R, et al. Predictive accuracy of lepidic growth subtypes in early-stage adenocarcinoma of the lung by quantitative CT histogram and FDG-PET. *Lung Cancer* 2018;125:14-21
26. Nishii K, Bessho A, Fukamatsu N, Ogata Y, Hosokawa S, Sakugawa M, et al. Statistical analysis of 18F-fluorodeoxyglucose positron-emission tomography/computed tomography ground-glass nodule findings. *Mol Clin Oncol* 2018;9:279-282
27. Lee HJ, Lee CH, Jeong YJ, Chung DH, Goo JM, Park CM, et al. IASLC/ATS/ERS international multidisciplinary classification of lung adenocarcinoma: novel concepts and radiologic implications. *J Thorac Imaging* 2012;27:340-353
28. Godoy MC, Naidich DP. Overview and strategic management of subsolid pulmonary nodules. *J Thorac Imaging* 2012;27:240-248
29. Shao X, Niu R, Jiang Z, Shao X, Wang Y. Role of PET/CT in management of early lung adenocarcinoma. *AJR Am J Roentgenol* 2020;214:437-445
30. Lee HY, Jeong JY, Lee KS, Yi CA, Kim BT, Kang H, et al. Histopathology of lung adenocarcinoma based on new IASLC/ATS/ERS classification: prognostic stratification with functional and metabolic imaging biomarkers. *J Magn Reson Imaging* 2013;38:905-913
31. Gormsen LC, Vendelbo MH, Pedersen MA, Haraldsen A,

https://doi.org/10.3348/kjr.2021.0455

Hjorthaug K, Bogsrud TV, et al. A comparative study of standardized quantitative and visual assessment for predicting tumor volume and outcome in newly diagnosed diffuse large B-cell lymphoma staged with 18F-FDG PET/CT. *EJNMMI Res* 2019;9:36
32. Castello A, Rossi S, Mazziotti E, Toschi L, Lopci E. Hyperprogressive disease in patients with non-small cell lung cancer treated with checkpoint inhibitors: the role of 18F-FDG PET/CT. *J Nucl Med* 2020;61:821-826
33. Del Gobbo A, Pellegrinelli A, Gaudioso G, Castellani M, Zito Marino F, Franco R, et al. Analysis of NSCLC tumour heterogeneity, proliferative and 18F-FDG PET indices reveals Ki67 prognostic role in adenocarcinomas. *Histopathology* 2016;68:746-751
34. Shen G, Ma H, Pang F, Ren P, Kuang A. Correlations of 18F-FDG and 18F-FLT uptake on PET with Ki-67 expression in patients with lung cancer: a meta-analysis. *Acta Radiol* 2018;59:188-195
35. Sauter AW, Winterstein S, Spira D, Hetzel J, Schulze M, Mueller M, et al. Multifunctional profiling of non-small cell lung cancer using 18F-FDG PET/CT and volume perfusion CT. *J Nucl Med* 2012;53:521-529
36. Nishimukai A, Inoue N, Kira A, Takeda M, Morimoto K, Araki K, et al. Tumor size and proliferative marker geminin rather than Ki67 expression levels significantly associated with maximum uptake of 18F-deoxyglucose levels on positron emission tomography for breast cancers. *PLoS One* 2017;12:e0184508
37. Incoronato M, Grimaldi AM, Cavaliere C, Inglese M, Mirabelli P, Monti S, et al. Relationship between functional imaging and immunohistochemical markers and prediction of breast cancer subtype: a PET/MRI study. *Eur J Nucl Med Mol Imaging* 2018;45:1680-1693
38. Morawitz J, Kirchner J, Martin O, Bruckmann NM, Dietzel F, Li Y, et al. Prospective correlation of prognostic immunohistochemical markers with SUV and ADC derived from dedicated hybrid breast 18F-FDG PET/MRI in women with newly diagnosed breast cancer. *Clin Nucl Med* 2021;46:201-205
39. Parent EE, Benayoun M, Ibeanu I, Olson JJ, Hadjipanayis CG, Brat DJ, et al. [18F]Fluciclovine PET discrimination between high- and low-grade gliomas. *EJNMMI Res* 2018;8:67
40. Chang CC, Cho SF, Chen YW, Tu HP, Lin CY, Chang CS. SUV on dual-phase FDG PET/CT correlates with the Ki-67 proliferation index in patients with newly diagnosed non-Hodgkin lymphoma. *Clin Nucl Med* 2012;37:e189-e195
41. Mu W, Jiang L, Zhang J, Shi Y, Gray JE, Tunali I, et al. Non-invasive decision support for NSCLC treatment using PET/CT radiomics. *Nat Commun* 2020;11:5228
42. Yip SS, Kim J, Coroller TP, Parmar C, Velazquez ER, Huynh E, et al. Associations between somatic mutations and metabolic imaging phenotypes in non–small cell lung cancer. *J Nucl Med* 2017;58:569-576
43. Zhang J, Zhao X, Zhao Y, Zhang J, Zhang Z, Wang J, et al. Value of pre-therapy 18F-FDG PET/CT radiomics in predicting EGFR mutation status in patients with non-small cell lung cancer. *Eur J Nucl Med Mol Imaging* 2020;47:1137-1146
44. Kim YI, Paeng JC, Park YS, Cheon GJ, Lee DS, Chung JK, et al. Relation of EGFR mutation status to metabolic activity in localized lung adenocarcinoma and its influence on the use of FDG PET/CT parameters in prognosis. *AJR Am J Roentgenol* 2018;210:1346-1351
45. Zhu L, Yin G, Chen W, Li X, Yu X, Zhu X, et al. Correlation between EGFR mutation status and F18 -fluorodeoxyglucose positron emission tomography-computed tomography image features in lung adenocarcinoma. *Thorac Cancer* 2019;10:659-664
46. Jiang L, Mino-Kenudson M, Roden AC, Rosell R, Molina MÁ, Flores RM, et al. Association between the novel classification of lung adenocarcinoma subtypes and EGFR/KRAS mutation status: a systematic literature review and pooled-data analysis. *Eur J Surg Oncol* 2019;45:870-876

 https://doi.org/10.3348/kjr.2021.0455